An Analysis of the Accuracy of Indirect Shaft Sensor for Synchronous Reluctance Motor

M. S. Arefeen, *Student Member, IEEE,* M. Ehsani, *Senior Member, IEEE,* and T. A. Lipo, *Fellow, IEEE*

Abstract—**This paper reports a rotor position sensing technique for synchronous reluctance motors (SynRM's) without using any discrete position sensors. An accuracy analysis of the new indirect SynRM position sensing scheme is presented. The analysis breaks down the position error to its fundamental causes in the position sensing scheme. The same basic approach can be taken to evaluate other SynRM rotor position sensing schemes.**

I. Introduction

SYNCHRONOUS reluctance motors (SynRM's) are suitable for many commercial drive applications because of their inherent simplicity and ruggedness. In particular, it has been shown that a properly designed SynRM drive with field oriented control can perform as well as an induction motor drive when the field weakening range is not too wide [1]–[3]. However, the need for a rotor position sensor for a vector controlled SynRM drive tends to compromise the natural cost and simplicity advantage of these motors. Therefore, it is very desirable to eliminate the discrete shaft sensors, while producing the necessary position information for the drive controller. This paper presents the results of accuracy analysis of a new indirect rotor position sensing scheme for SynRM's, which has been developed in the Power Electronic Laboratory at Texas A & M University. The developed rotor position sensing scheme provides position information at the zero crossings within one electrical cycle of a three-phase machine, this technique provides six rotor position samples. However, these six samples per electrical cycle are not sufficient for any high-performance application. In order to increase the rotor position sampling rate, the controller must employ extrapolation to derive rotor position information between two zero crossings of the phase current. Stator flux information can be used for this extrapolation purpose. However, an investigation of performance and fundamental accuracy of our six-sample method is the topic of specific interest of this paper.

Paper IPCSD 94-38, approved by the Industrial Drives Committee of the IEEE Industry Applications Society for presentation at the 1993 Industry Applications Society Annual Meeting, Toronto, Canada, October 2–8. Manuscript released for publication April 11, 1994.

M. S. Arefeen and M. Ehsani are with the Power Electronics Laboratory, Department of Electrical Engineering, Texas A & M University, College Station, TX 77843.

T. A. Lipo is with the Department of Electrical and Computer Engineering, University of Wisconsin-Madison, 1415 Johnson Drive, Madison, WI 53706.

IEEE Log Number 9404066.

II. Indirect Position Sensing in Synchronous Reluctance Motor

The SynRM possesses unique features which make position sensing much simpler and more reliable than either conventional squirrel cage induction machines or switched reluctance machines. In contrast to the induction machine, the SynRM possesses saliency which permits the rotor position to be sensed, since the inductance per phase is a function of rotor position. This allows sensing position at zero speed, which is impossible for an induction machine. Second, in contrast to the switched reluctance motor, the stator windings of the SynRM are magnetically coupled. Hence voltages are induced in the stator windings which are open circuited. This allows sensing of the emf. These two features in combination can be used to obtain rotor position information for the SynRM [4].

The rotor position information of a SynRM will be obtained by employing a special switching technique for the current regulated pulse width modulated (CRPWM) converter. In a regular CRPWM converter, the pulse switches are normally turned on and off in order to make the individual phase currents follow the desired reference within a desired band. However, in the modified switching technique, both of the switches of that phase are turned off when the current of a particular phase, e.g., phase A, crosses zero. The remaining two phases (in this case phases B and C) are excited in series by turning on alternate pairs of switches [the lower switch of phase B and the upper switch of phase C (Fig. 1(a)) or the lower switch of phase C and the upper switch of phase B (Fig. 1(b))]. This modified switching pattern will extend the zero crossing of phase A for a short interval. Although current of phase A during this extended zero-crossing period will be zero, a voltage will be induced in phase A due to the currents in the other two phases. The induced voltage in phase A can be expressed as [4],

$$V_{\text{ind}} = \frac{d}{dt}(L_{ab} i_{bs} + L_{ac} i_{cs}), \tag{1}$$

where L_{ab} and L_{ac} are the mutual inductances between phases A and B and between phases A and C, respec-

tively. Since phase B and phase C are now effectively in series, $i_{bs} = -i_{cs}$ and $d/dt(i_{bs}) = -d/dt(i_{cs})$, and (1) becomes

$$V_{\text{ind}} = (L_{ab} - L_{ac})\frac{d}{dt}i_{bs} + i_{bs}\frac{d}{dt}(L_{ab} - L_{ac}). \quad (2)$$

Since the mutual inductances depend on rotor positions [5], (2) can be written as

$$V_{\text{ind}} = K_1 \sin(2\theta_r) + K_2 \cos(2\theta_r), \quad (3)$$

where

$$K_1 = -\left(2L_B \sin\frac{2\pi}{3}\right)\frac{d}{dt}i_{bs},$$

$$K_2 = -\left(4L_b\omega_r \sin\frac{2\pi}{3}\right)i_{bs},$$

and L_B is a physical parameter of the motor.

In (3), ω_r is the rotor speed in electrical rad/s, which is equal to the frequency applied to the stator. Thus by knowing the induced voltage V_{ind}, the slope and the instantaneous value of the current, i_{bs}, and using ω_r, it is theoretically possible to compute the instantaneous value of the rotor position θ_r.

Fig. 2 shows a measured trace of phase A current with one extended zero-crossing interval. During the extended zero-crossing period of phase A current, phases B and C of the converter are switched in a special diagnostic manner. This diagnostic switching interval consists of following a constant reference current, in each phase, by means of hysteresis control. The level of constant reference currents in phases B and C are exactly the instantaneous value of these currents, respectively, at the instant of phase A current zero crossing. Fig. 3 shows the constant pulse width modulation of phase B during that extended zero crossing of phase A. The sequence of coupled voltage pulses, shown in Fig. 4, have the instantaneous rotor angle encoded in their amplitudes, according to (3). Each individual pulse amplitude shown in Fig. 4 can deliver one rotor angle sample by means of a look-up table. The table contains the inverse function of (3), solved for θ_r, in discrete form. For implementation, the voltage pulses are fed directly to a microcontroller (INTEL 80C196KR), having a 16-MHz clock speed, in order to get a highly accurate position information.

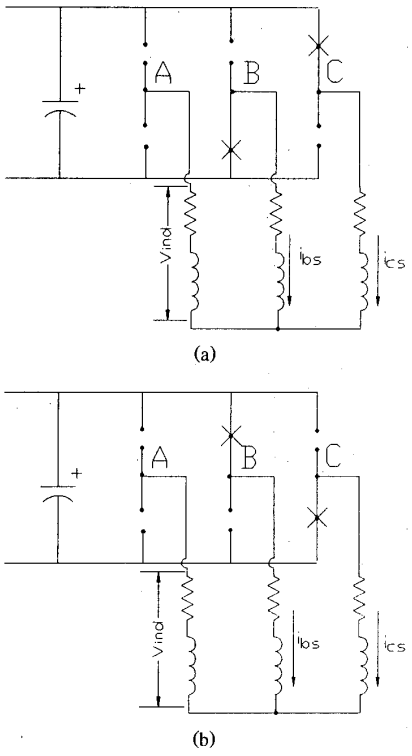

Fig. 1. Circuit configurations during the extension of the zero-crossing period of phase A current.

However, this extension of the zero-crossing period of one phase and constant pulse width modulation of the remaining two phases will introduce lower-order harmonics in stator currents. But these lower-order harmonics introduced by a typical extended zero-crossing window (200 μs, which is enough to record the required voltage pulses using microcontroller INTEL196KR) are insignificant compared to the fundamental component of the stator current. This is shown in Tables I and II giving the ratio between fundamental and harmonic currents.

It is important to note that the proposed technique can determine the rotor position even at zero speed. At zero speed all phase currents are zero. This provides one with the opportunity of sequentially inducing the diagnostic pwm signals on any pair of phases while the current in the other phase is zero. The additional advantage is that the zero crossing can be made to persist for as long as one wishes the diagnostic interval to be. Furthermore, the speed term $i_{bs}(d/dt)(L_{ab} - L_{ac})$ in (2) is eliminated in the look-up table for θ_r, which can now be derived from the simple form given below:

$$V_{\text{ind}} = (L_{ab} - L_{ac})\frac{d}{dt}i_{bs}. \quad (4)$$

Easily measurable noise-free induced voltage can be obtained with a phase current which has low amplitude, high frequency, and zero average value. Thus estimation of the rotor positions at zero speed will not produce any torque ripple. In order to calculate the starting rotor position of the experimental drive, three pairs of phases were diagnostically energized in sequence and the induced voltage was read across the unenergized phase, as previously explained. Fig. 5 shows the diagnostic constant zero current regulation flowing through the phases B and C of the experimental drive, where phases B and C were pulsed at 4.44 kHz diagnostic current. Fig. 6 shows the voltage induced across phase A during that diagnostic interval. A strong, easily measurable signal is clearly evident.

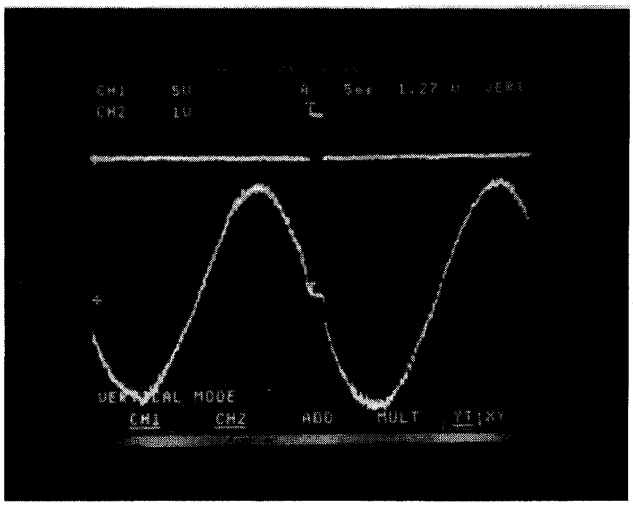

Fig. 2. Lower trace: phase A current with extended zero-crossing period. Upper trace: control pulse for disconnecting phase A.

III. Error Analysis of the New Technique

The error analysis of the proposed technique is divided into two major sections. First, the error in individual rotor samples is calculated. This may be called the "sample error." Second, the error introduced due to extrapolation of the rotor samples between two zero crossings of phase currents is calculated. This may be called "intersample error." An expression for the drive acceleration is developed, so that, depending on the operating and load conditions, the maximum allowable drive acceleration can be estimated, without making the intersample errors greater than the individual sample error.

IV. Error in Each Individual Sample

The error in rotor samples comes from the quantization error in the measurements of induced voltage, phase current, and current slope. Thus, the worst case of the position estimation will occur at the worst case of the quantization error:

$$\Delta\theta_r = \Delta\theta_{sq}, \tag{5}$$

where $\Delta\theta_{sq}$ = quantization sample error (mechanical degrees) due to measurement errors.

A. Quantization Error, $\Delta\theta_{sq}$, Calculation

The variation of induced voltage is a nonlinear function of rotor position and only the average sample error in the digitizing process can be obtained. The quantization error results from conversion of the induced voltage V_{ind}, the current slope di_b/dt, and the phase current i_b (see (3)) to their integer digital representation, and is always equal to 0.5 least significant bit (LSB). Using (3), the rotor position θ_r can be written as a function of the measured variables: $\theta_r = \theta(V_{\text{ind}}, K_1, K_2)$. The quantization error in θ_r can be approximated by the first terms of its Taylor expansion in terms of quantization errors in the variables:

$$\Delta\theta_{sq} = \frac{\partial\theta_r}{\partial V_{\text{ind}}}\Delta V_{\text{ind}} + \frac{\partial\theta_r}{\partial K_1}\Delta K_1 + \frac{\partial\theta_r}{\partial K_2}\Delta K_2, \tag{6}$$

where ΔV_{ind}, ΔK_1, and ΔK_2 are the individual variable quantization errors which depend on the A/D converter resolution and the full-scale range of the individual variables. The above expression gives the worst case error in terms of quantization error alone, where it is assumed that the accuracy of the analog voltage and current probes and their interface electronics are less than their respective quantization error. If $V_{\max}$ is the maximum measured induced voltage, then the quantization error for the induced voltage measurement, ΔV_{ind}, becomes

$$\frac{V_{\max}}{2^n},$$

where n is the number of output bits of the A/D converter. Similarly, with the maximum phase current $I_{\max}$, the quantization error for current measurement Δi becomes

$$\frac{I_{\max}}{2^n}.$$

The input variable K_1 depends on the current slope, which makes the error ΔK_1 dependent on the current sampling rate. The slope of the phase current during the extended zero-crossing period is calculated by measuring the phase currents at the switching instants of the phase pair and then dividing the difference of the measured currents by the time interval between the switching instants. If i_1 and i_2 are the currents at the two switching instants of the phase current, then with the quantization

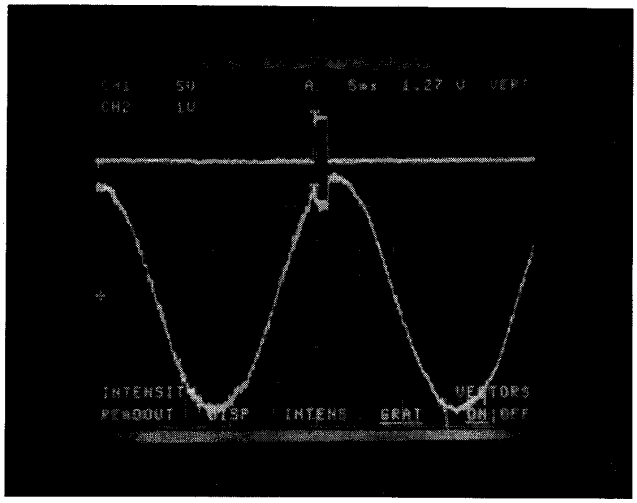

Fig. 3. Phase B current (lower trace) goes into constant pulse width modulation during the extended zero crossing of phase A.

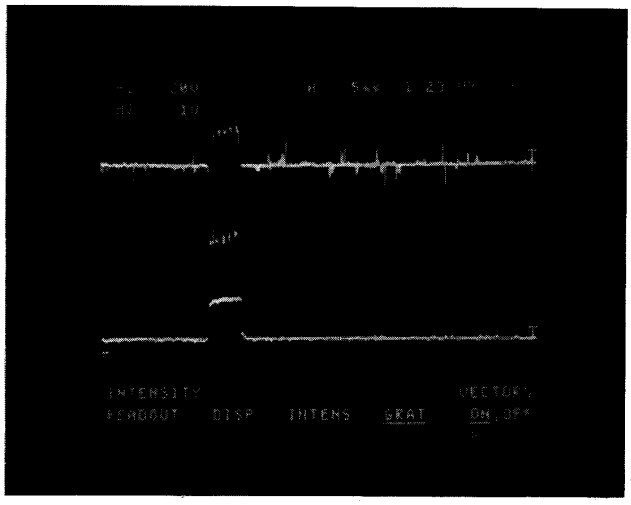

Fig. 4. Induced voltage measured in phase A. Upper trace: induced voltage. Lower trace: control pulse.

TABLE I
HARMONICS IN PHASE A CURRENT

Harmonic No.	Harmonic/Funda. (%)
2	2.5
3	2.4
4	1.6
>5	<1.5

TABLE II
HARMONICS IN PHASES B AND C CURRENT

Harmonic No.	Harmonic/Funda. (%)
2	1.7
5	1.6
7	1.5
>9	<1.3

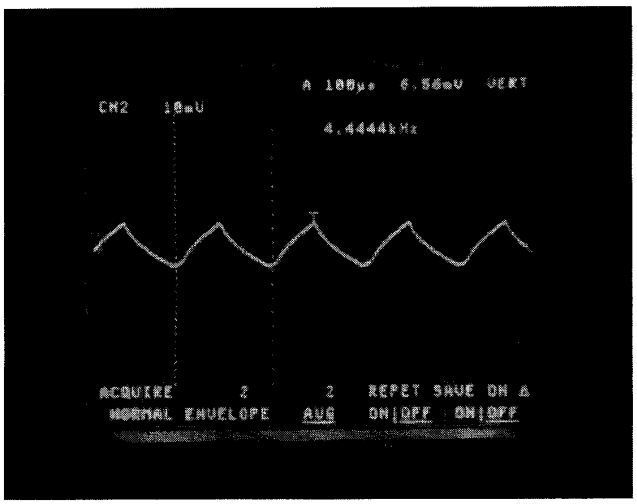

Fig. 5. Diagnostic current flowing through the phases B and C during the start-up operation (10 mV/div, 100 μs/div).

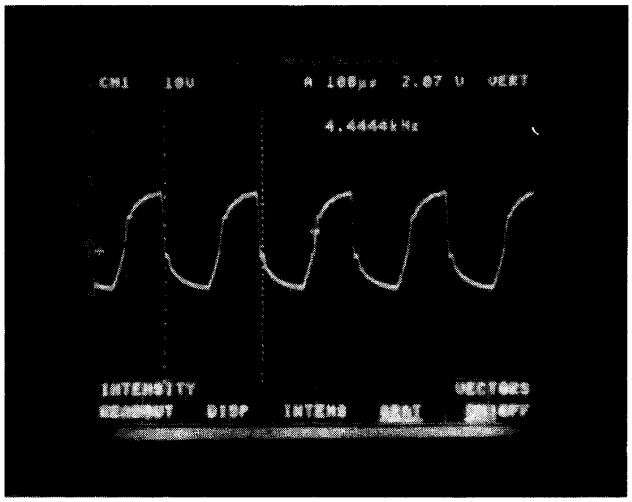

Fig. 6. Induced voltage in phase A during the start-up operation (10 V/div, 100 μs/div).

error of Δi, the worst case current difference becomes

$$i_2 - i_1 + 2\Delta i.$$

Consequently, the worst case error for current slope measurement (assuming linear current variation between i_1 and i_2) becomes

$$\frac{2\,\Delta i}{1/(2f_s)} = 4\Delta i f_s,$$

where f_s is the PWM switching frequency during the extended zero-crossing period of the phase current. This error in current slope measurement will contribute to the error ΔK_1, which can be written as

$$\Delta K_1 = -\left(2L_B \sin\frac{2\pi}{3}\right)\Delta\left(\frac{d}{dt}i\right) = -\left(2L_B \sin\frac{2\pi}{3}\right)\cdot 4\Delta i f_s.$$

The quantization error of the parameter K_2 depends on the current quantization error and can be written as

$$\Delta K_2 = -\left(4L_B\omega_r \sin\frac{2\pi}{3}\right)\Delta i.$$

Using (6), the quantization error for the individual rotor samples can be expressed as

$$\Delta\theta_{sq} = \frac{\partial\theta_r}{\partial V_{\text{ind}}}\Delta V_{\text{ind}} + \frac{\partial\theta_r}{\partial K_1}\left(-8L_B \sin\frac{2\pi}{3} f_s \Delta i\right) + \frac{\partial\theta_r}{\partial K_2}\left(-4L_B\omega_r \sin\frac{2\pi}{3}\Delta i\right). \quad (7)$$

Eq. (7) can now be expressed in terms of the maximum magnitude of the input variables and the resolution of the

A/D converter as

$$\Delta\theta_{sq} = \frac{\partial\theta_r}{\partial V_{\text{ind}}}\frac{V_{\max}}{2^n} + \frac{\partial\theta_r}{\partial K_1}\left(-8L_B \sin\frac{2\pi}{3} f_s \frac{I_{\max}}{2^n}\right) + \frac{\partial\theta_r}{\partial K_2}\left(-4L_B\omega_r \sin\frac{2\pi}{3}\frac{I_{\max}}{2^n}\right). \quad (8)$$

Let us now calculate the quantization error of the individual samples according to the data obtained from one of our experiments. The experimental machine has an induction motor stator and rotor type described in [1]–[3]. In our experiment, the maximum measured induced voltage was 80 V and our A/D converter had an 8-bit resolution. This makes the quantization error of the induced voltage ΔV_{ind} equal to 0.31 V. The rated phase current of the experimental motor is 10 A, making the quantization error for the current measurement equal to 0.04 A, which consequently makes the error ΔK_2 equal to 0.18 HA/sec at 1000 rpm. With 0.04 A of current quantization error and 8 kHz of PWM frequency, the worst case error in current slope measurement is 1280 A/sec, which makes the error ΔK_1 equal to 7.58 HA/sec. The maximum $\partial\theta_r/\partial V_{\text{ind}}$, $\partial\theta_r/\partial K_1$, and $\partial\theta_r/\partial K_2$ can be found from analytically or numerically maximizing them in the possible range of the three dimensions i, i^0, and V_{ind}. The numerical value of the worst case position error is found by substituting system parameters L_B, n, $V_{\max}$, $I_{\max}$ and the ranges of i, i^0, and V_{ind}. Using (8), the worst case error for rotor position estimation, $\Delta\theta_{sq}$ (considering worst case of all the parameters), is found to be equal to or less than 0.80 mechanical degrees.

It should be mentioned that the estimated quantization error can be lowered by using 10-bit A/D conversion of the analog signals ((8)). However, the conversion time required for a 10-bit A/D will be longer.

The estimated quantization error will now be used in the next section to keep the intersample error within the individual sample error.

V. Error Calculation due to Extrapolation

The proposed technique provides rotor samples at every zero crossing of the phase currents. Thus, extrapolation technique has to be applied in order to estimate rotor position between two zero crossings. A linear extrapolation will be sufficient to estimate rotor positions during the constant speed operation of the drive. However, during the acceleration period of the drive, linear extrapolation will introduce errors in rotor position estimation. Thus, acceleration of the drive has to be limited, so that the rotor estimation error between two zero crossings does not exceed a predefined error margin. In this analysis $\Delta\theta_{\text{sample}}$, which is equal to $\Delta\theta_{sq}$, is taken as the acceptable margin of error for extrapolation between two zero crossings.

Suppose the rotor speed ω^* is constant and let the rotor position be θ_1 at time t_1 (see Fig. 7), then using the linear extrapolation, the new rotor position θ_2 at time t_2 can be written as

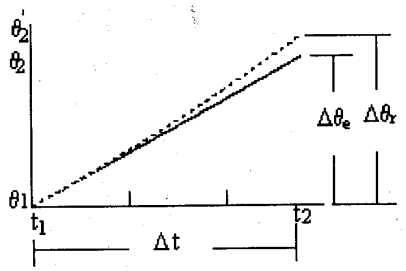

Fig. 7. Rotor position variation with and without drive acceleration.

$$\theta_2 = \int_{t_1}^{t_2}\omega^* dt + \theta_1,$$

$$\theta_2 = \omega^*\Delta t + \theta_1, \quad (9)$$

where Δt is the time interval between two zero crossings of the phase current. Thus the change in rotor angle, $\Delta\theta_e$, in the interval Δt is

$$\Delta\theta_e = \omega^*\Delta t. \quad (10)$$

Now let us consider a constant acceleration K for the motor. Then, the new rotor speed ω after time t can be written as

$$\omega = \omega^* + Kt. \quad (11)$$

With this new acceleration K, the new rotor position θ_2' at the end of the time interval can be written as (see Fig. 7)

$$\theta_2' = \frac{1}{2}K(\Delta t)^2 + \omega^*\Delta t + \theta_1. \quad (12)$$

Thus, the rotor angle variation with this acceleration is

$$\Delta\theta_r = \tfrac{1}{2}K(\Delta t)^2 + \omega^*\Delta t. \quad (13)$$

To keep this angle variation within an acceptable margin, we can limit the acceleration of the drive by defining the boundary condition as

$$\Delta\theta_r - \Delta\theta_e \le \Delta\theta_{\text{sample}},$$

$$\tfrac{1}{2}K(\Delta t)^2 + \omega^*\Delta t - \omega^*\Delta t \le \Delta\theta_{\text{sample}},$$

$$K \le 2\cdot\frac{\Delta\theta_{\text{sample}}}{(\Delta t)^2}, \quad (14)$$

$$K \le 72\cdot\Delta\theta_{\text{sample}}\cdot f_e^2, \quad (15)$$

where $\Delta t = 1/(6f_e)$ and f_e is the electrical frequency of the drive.

The following observations can be made from the drive acceleration given by (14) and (15):

- The allowable acceleration is proportional to the error margin.
- Starting acceleration has to be low due to the long time interval between two consecutive zero crossings (long Δt).

- High acceleration is possible at high-speed operation (short Δt).

In the previous section, the $\Delta\theta_r$ was calculated to be 0.80° at the operating frequency of 33 Hz. The operating speed was 1000 rpm. For this particular case the acceptable acceleration becomes

$$K = 1090 \text{ rad/sec}^2.$$

The following equation, along with (14) or (15), can be used to identify the drives for which this new technique is suitable for rotor sensing with a desired accuracy:

$$T = \frac{WR^2}{308} \frac{(\text{rpm}_2 - \text{rpm}_1)}{\Delta t} \quad \text{lb-ft}, \qquad (16)$$

where T is the torque required for the acceleration between two speeds rpm_1 and rpm_2. WR^2 is the inertia of the system in lb-ft^2.

Eqs. (15) and (16) show that the applicability of the technique depends on the system inertia and the motor torque. A suitable system for this technique will have a high enough system inertia to keep the acceleration low during operation. However, the system acceleration can increase at higher speeds as shown by (14). Pump, fan, and compressor applications satisfy this low starting torque and high-inertia requirements of the new technique. For example, a typical 50-hp compressor drive ($WR^2 = 135$ lb-ft^2) with a starting torque of 230 lb-ft has a starting acceleration of 50 rad/sec^2, which is low enough for the new technique to provide accurate rotor position samples. The acceleration can increase as the drive gradually picks up speed. Thus the extrapolation technique, without any modifications, is suitable for fan, pump, and compressor applications using large machines (> 50 hp).

VI. Conclusion

The error in rotor position estimation resulting from the application of the proposed technique is calculated. The individual sample error at the phase current zero crossings comes from the quantization error of the induced voltage and the quantization and the sampling rate errors of the phase current. It is shown that the rotor position sensor, as we have at the present, is adequate for $\leq 1°$ accuracy in rotor position sensing during the extended zero-crossing periods of the phase currents.

In order to keep the intersample error within this error margin ($\leq 1°$), an expression for the drive acceleration is developed, which shows the relationship between the intersample error and the other system components. It is found that the proposed technique is suitable for slowly changing speeds, e.g., in pump and fan applications. However, the proposed technique can easily be applied to fast speed changing applications, when some other means is adopted (for example, flux estimation), to estimate the rotor position between the zero crossings of the phase currents.

References

[1] T. A. Lipo, "Synchronous reluctance machines—A viable alternative for ac drives?" *Electr. Mach. Power Syst.*, vol. 19, pp. 659–671, 1991.

[2] L. Xu, X. Xu, T. A. Lipo, and D. W. Novotny, "Vector control of a synchronous reluctance machine including saturation and iron loss," *Conf. Rec. IEEE-IAS Ann. Mtg.*, 1990, pp. 359–364.

[3] T. Matsua and T. A. Lipo, "Field oriented control of synchronous reluctance machine," in *Proc. IEEE Power Electron. Specialist's Conf.*, 1993, pp. 425–431.

[4] M. Arefeen, M. Ehsani, and T. A. Lipo, "Elimination of discrete position sensor for synchronous reluctance motor," in *Proc. IEEE Power Electron. Specialist's Conf.*, 1993, pp. 440–445.

[5] P. C. Krause, *Analysis of Electric Machinery*. New York: McGraw-Hill, 1986.

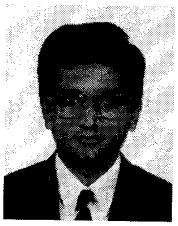

M. S. Arefeen received the B.S. degree in electrical engineering from Bangladesh University of Engineering & Technology, Dhaka, Bangldesh in 1987, and the M.S. degree from Texas A & M University, College Station, TX, in 1990.

He is currently a Research Assistant in the Department of Electrical Engineering at Texas A & M University, and is working toward the Ph.D. degree in the area of power electronics. His research interests are in power electronics, motor drives, and their control systems.

Mehrdad Ehsani (S'70–M'81–SM'83) received the B.S. and M.S. degrees from the University of Texas at Austin in 1973 and 1974, respectively, and the Ph.D. degree from the University of Wisconsin-Madison in 1981, all in electrical engineering.

From 1974 to 1977 he was with the Fusion Research Center, University of Texas, as a Research Engineer. From 1977 to 1981 he was with Argonne National Laboratory, Argonne, IL, as a Resident Research Associate, while simultaneously doing the doctoral work at the University of Wisconsin-Madison in energy systems and control systems. Since 1981 he has been at Texas A & M University, College Station, TX, where he is now the Halliburton chaired Professor of Electrical Engineering and Director of Texas Applied Power Electronics Center (TAPC). He is the author of over 95 publications in pulsed-power supplies, high-voltage engineering, power electronics, and motor drives, and is the recipient of the Prize Paper Award in Static Power Converters and motor drives at IEEE-Industry Applications Society 1985, 1987, and 1992 Annual Meetings. In 1984 he was named the Outstanding Engineer of the Year by Texas Society of Professional Engineers. He is also the co-author of a book on converter circuits for superconductive magnetic energy storage and a contributor to an IEEE Guide for Self-Commutated Converters and other monographs. He is the author of seven U.S. patents. His current research work is in power electronics, motor drives, hybrid vehicles, and their control systems.

Dr. Ehsani is a member of IEEE Power Electronics Society AdCom, Chairman of PELS Educational Affairs Committee, IEEE Industry Applications Society Executive Council, past Chairman of IEEE-IAS Industrial Power Converter Committee, and Chairman of the IEEE Myron Zucker Student-Faculty Grant program. He was the General Chair of IEEE Power Electronics Specialist Conference for 1990 and was an IEEE Industrial Electronics Distinguished Speaker. He is also a Registered Professional Engineer in the State of Texas.

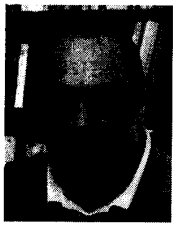

Thomas A. Lipo (M'64–SM'71–F'87) is a native of Milwaukee, WI. He received the B.E.E. and M.S.E.E. degrees from Marquette University, Milwaukee, WI in 1962 and 1964 and the Ph.D. degree in electrical engineering from the University of Wisconsin in 1968.

From 1969 to 1979 he was an Electrical Engineer in the Power Electronics Laboratory of Corporate Research and Development of the General Electric Company, Schenectady, NY. He became Professor of Electrical Engineering at Purdue University in 1979 and in 1981 he joined the University of Wisconsin in the same capacity, where he is presently the W. W. Grainer Professor for Power Electronics and Electrical Machines.

In 1986 Dr. Lipo received the Outstanding Achievement Award from the IEEE Industry Applications Society for his contributions to the field of ac drives, and in 1990 he received the William E. Newell Award of the IEEE Power Electronics Society for contributions to the field of power electronics. He has served in various capacities for three IEEE Societies. He was Chairman of the Industrial Drives Committee of IAS during 1986–1987, Chairman of the Industrial Power Conversion System Department of IAS in 1989, and has been an IAS Executive Committee member since 1990. He is currently serving as the President of the IEEE Industry Applications Society.